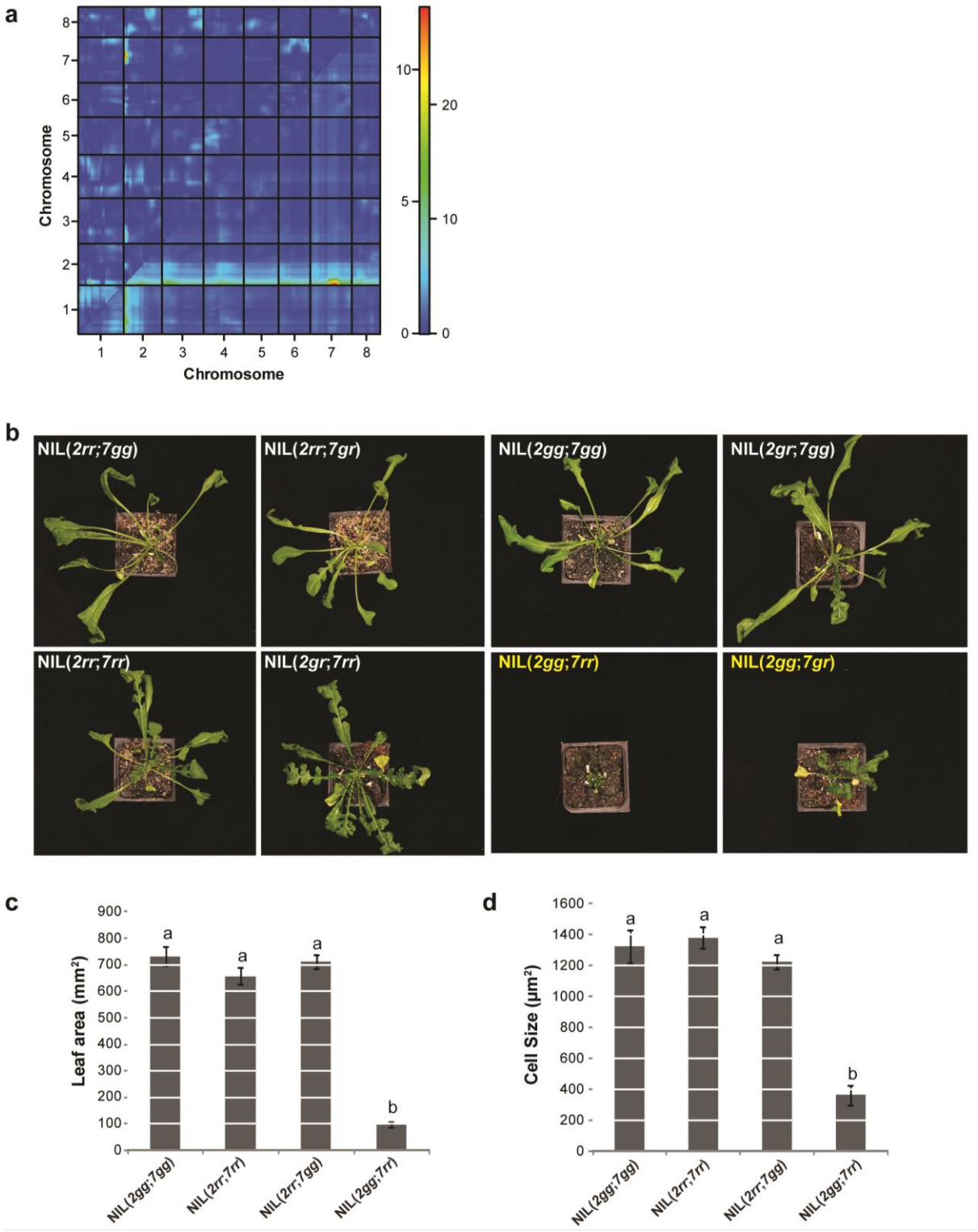


**Supplementary Figure 1: Characterisation of the incompatible interaction in *C. grandiflora* x *C. rubella* hybrids.**

**a** Results of two-dimensional QTL mapping for the incompatible phenotype. The full LOD score is shown below the diagonal, the interaction LOD score above. Colour scale refers to interaction LOD

score (left) and full LOD score (right). This QTL experiment has been performed using the phenotypic average values of 10 replicates for 142 RILs.

**b** Phenotypes of NIL plants with the indicated genotypes. Yellow font indicates incompatible phenotypes.

**c,d** Leaf area (**c**) and leaf-cell area (**d**) in the indicated genotypes. Values are mean ± s.e.m. of 10 and 4 leaves respectively per genotype, respectively. Letters indicate significant differences as determined by Tukey's HSD test ($\alpha$ =0.05).

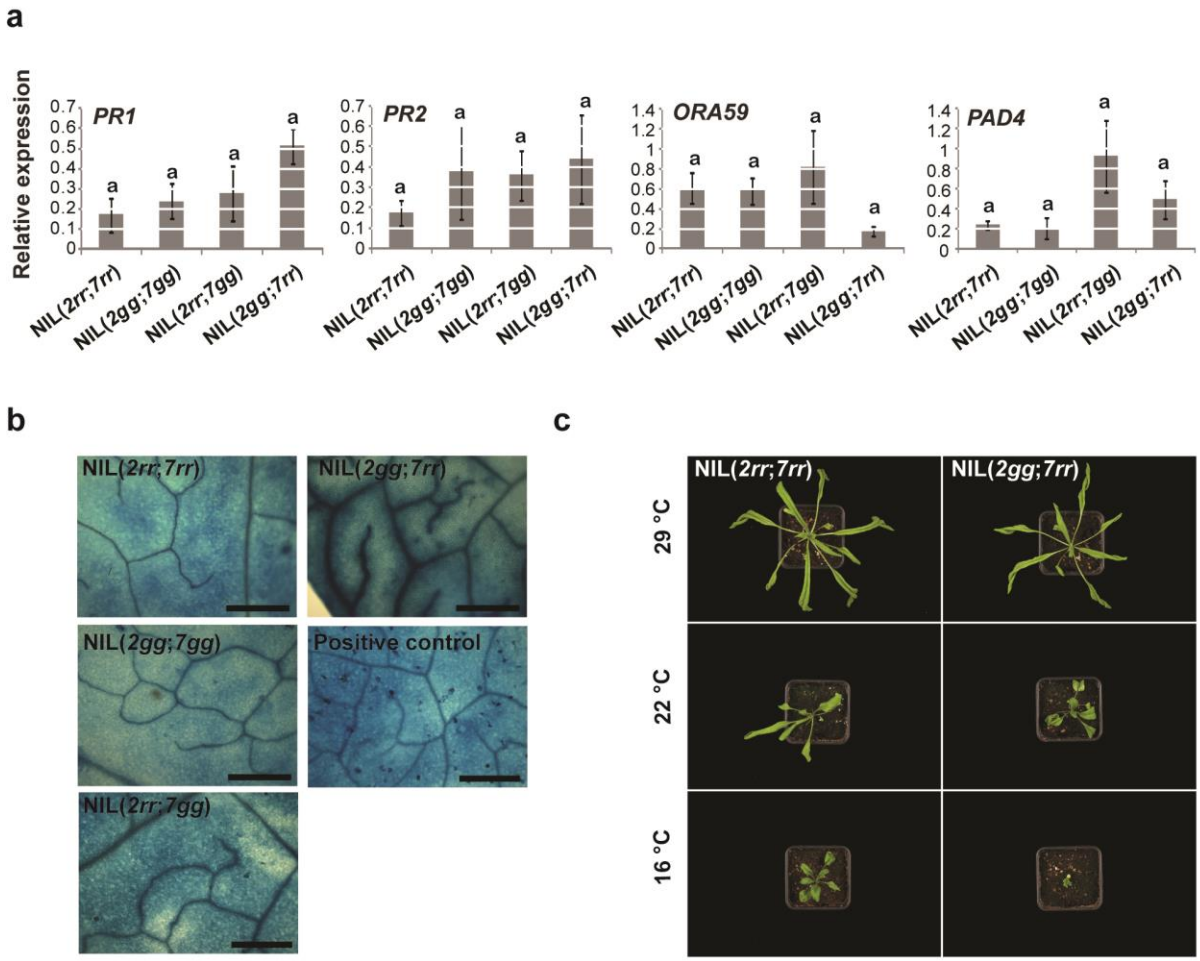


**Supplementary Figure 2: Characterization of the constitutive immune response in incompatible hybrids.**

**a** Expression of the indicated immune-response markers determined by qRT-PCR normalized to *Capsella TUB6*. Mean ± s.e.m. of three biological replicates is shown. Letters indicate significant differences as determined by Tukey's HSD test ($\alpha$ =0.05).

**b** Trypan Blue staining of leaves from the indicated genotype fails to detect ectopic necrosis in incompatible hybrids. Positive control is an early senescent leaf.

**c** The incompatible phenotype in NIL(*2gg; 7rr*) plants (right) can be rescued by growth at elevated temperatures as compared to compatible control plants (left).

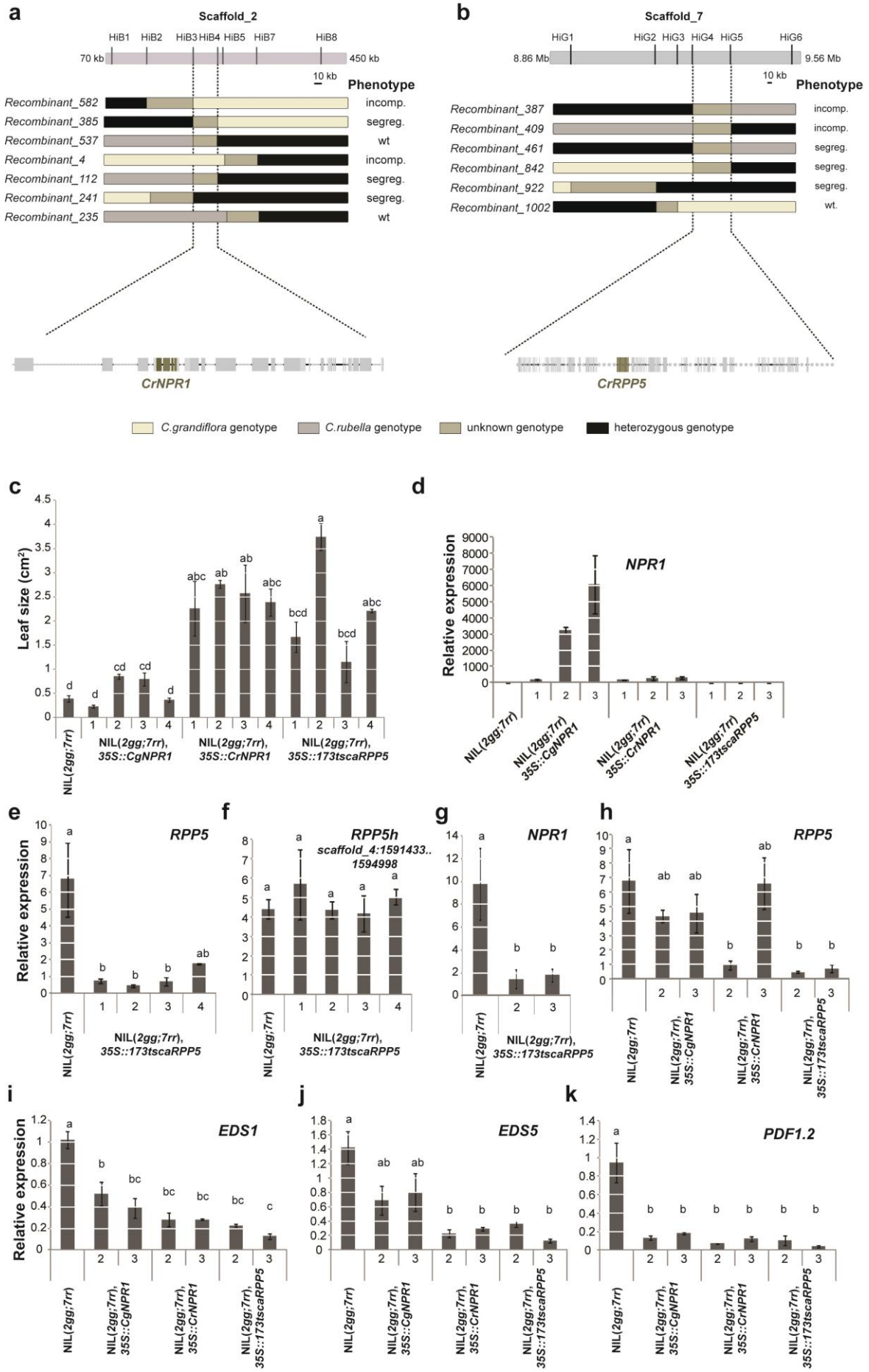
a
Scaffold_2
HiB1 HiB2 HiB3 HiB4 HiB5 HiB7 HiB8
70 kb
450 kb
10 kb
Phenotype
Recombinant_582 incomp.
Recombinant_385 segreg.
Recombinant_537 wt
Recombinant_4 incomp.
Recombinant_112 segreg.
Recombinant_241 segreg.
Recombinant_235 wt
CrNPR1
b
Scaffold_7
HiG1 HiG2 HiG3 HiG4 HiG5 HiG6
8.86 Mb
9.56 Mb
10 kb
Phenotype
Recombinant_387 incomp.
Recombinant_409 incomp.
Recombinant_461 segreg.
Recombinant_842 segreg.
Recombinant_922 segreg.
Recombinant_1002 wt.
CrRPP5
C.grandiflora genotype
C.rubella genotype
unknown genotype
heterozygous genotype
c
Leaf size (cm²)
NIL(2gg;7rr)
NIL(2gg;7rr), 35S::CgNPR1
NIL(2gg;7rr), 35S::CrNPR1
NIL(2gg;7rr), 35S::173tscaRPP5
d
Relative expression
NPR1
e
RPP5
f
RPP5h
scaffold_4:1591433..1594998
g
NPR1
h
RPP5
i
EDS1
j
EDS5
k
PDF1.2

**Supplementary Figure 3: Fine-mapping of the incompatible loci and transgenic rescue of the incompatible phenotype.**

**a, b** Location of markers used for mapping (top), genotypes and associated phenotypes of informative recombinants (middle) and annotated genome structure in the QTL2 (**a**) and QTL7 regions (**b**). Rectangles in the genome annotation represent exons, solid lines are introns and dotted lines show intergenic sequences.

**c** Leaf size in the indicated genotypes. Values are means ± s.e.m. from 4 leaves per genotypes. Numbers indicated independent transgenic lines for the same construct. Letters indicate significant differences as determined by Tukey's HSD test ($\alpha = 0.05$).

**d-k** Expression of *NPR1* (**d,g**), *RPP5* (**e,h**) and its closest *Capsella* paralogue *RPP5h* (**f**), and of immune-response markers *EDS1* (**i**), *EDS5* (**j**) and *PDF1.2* (**k**) determined by qRT-PCR normalized to *Capsella TUB6*. Mean ± s.e.m. of three (**d-f**) or four (**g-k**) biological replicates is shown. Letters indicate significant differences as determined by Tukey's HSD test ($\alpha = 0.05$). Numbers indicated independent transgenic lines for the same construct as in (**c**).

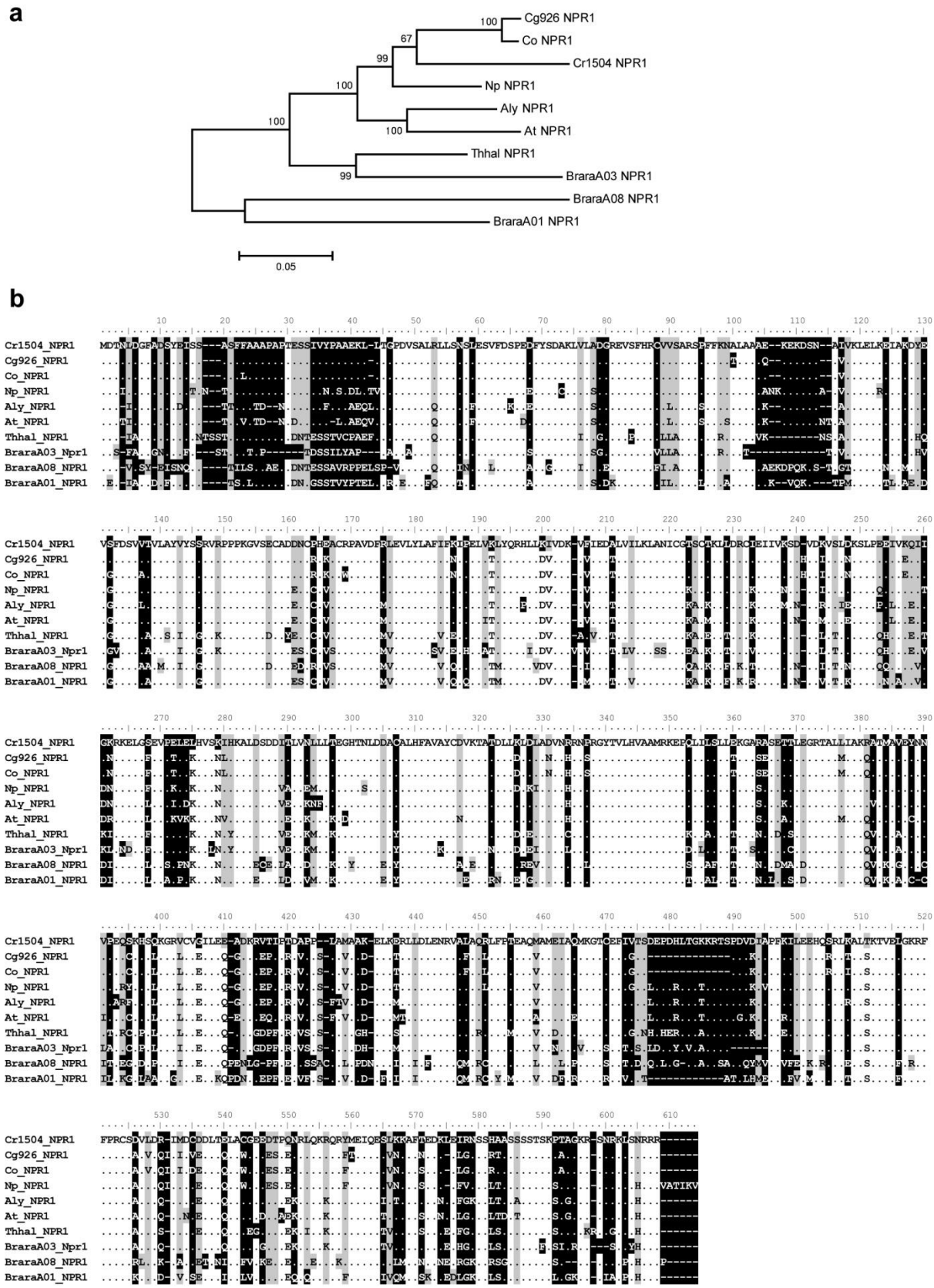


**Supplementary Figure 4: *NPR1* phylogeny in Brassicaceae**

**a, b** Phylogenetic tree (**a**) and protein sequence alignment (**b**) of NPR1 orthologues from different Brassicaceae. Identical amino acids are indicated by dots; conservative changes by grey, non-conservative changes by black shading. Aly: *Arabidopsis lyrata*, Ath: *A. thaliana*, Brara: *Brassica rapa*, Np: *Neslia paniculata*, Thhal: *Thelungiella halophila*.

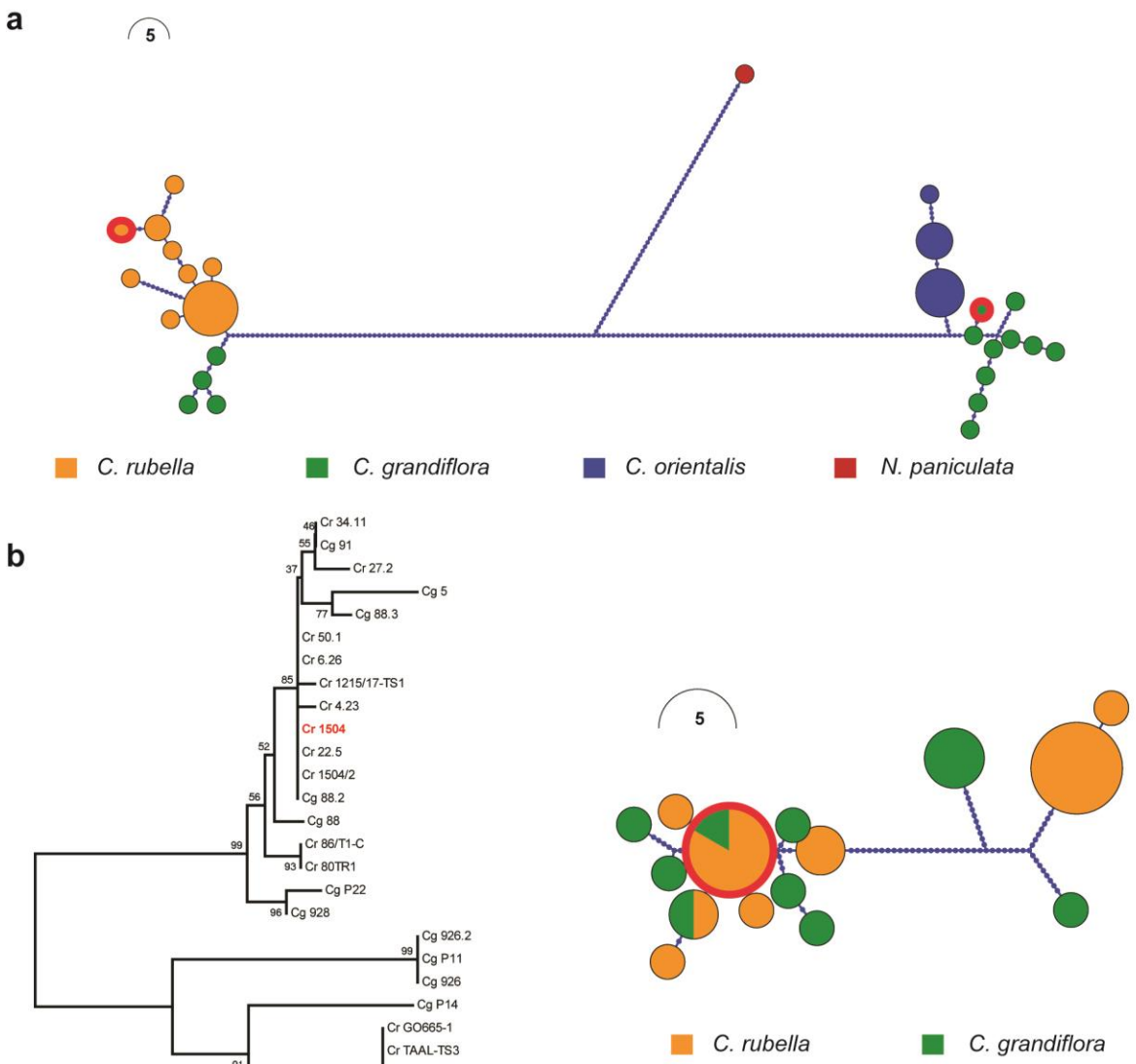
a
5
C. rubella
C. grandiflora
C. orientalis
N. paniculata
b
Cr 34.11
Cg 91
Cr 27.2
Cg 5
Cg 88.3
Cr 50.1
Cr 6.26
Cr 1215/17-TS1
Cr 4.23
Cr 1504
Cr 22.5
Cr 1504/2
Cg 88.2
Cg 88
Cr 86/T1-C
Cr 80TR1
Cg P22
Cg 928
Cg 926.2
Cg P11
Cg 926
Cg P14
Cr GO665-1
Cr TAAL-TS3
Cr 1377/5
Cr 23.9
Cr 49.5
Cr 8.5
Cr 39.1-TS1
Cr 1209/26-TS4
0.005
5
C. rubella
C. grandiflora
c
Cr
Cg
Co
Np
At
Al
Th
Br
10 kb
A01
A03
A08

**Supplementary Figure 5: Haplotype structure of *NPR1* and *RPP5* in *C. grandiflora* and *C. rubella*.**

**a** Haplotype network of *NPR1* in *C. grandiflora* (green), *C. rubella* (yellow), *C. orientalis* (blue) and *N. paniculata* (red). Red outlines indicate the *NPR1* haplotypes segregating in the RIL population. Analysis is based on resequencing of a 700 bp fragment.

**b** Neighbor-joinng phylogenetic tree of *RPP5* haplotypes from different *C. grandiflora* and *C. rubella* accessions (left) and corresponding haplotype network (right). Analysis is based on resequencing of an 800 bp fragment. Numbers indicated bootstrap support from 1,000 runs.

**c** Genome structure of *RPP5* region in Brassicaceae. Colours indicate syntenic genes. The phylogenetic tree shows known evolutionary relationships between the species. Corresponding regions from the three *B. rapa* subgenomes are shown.

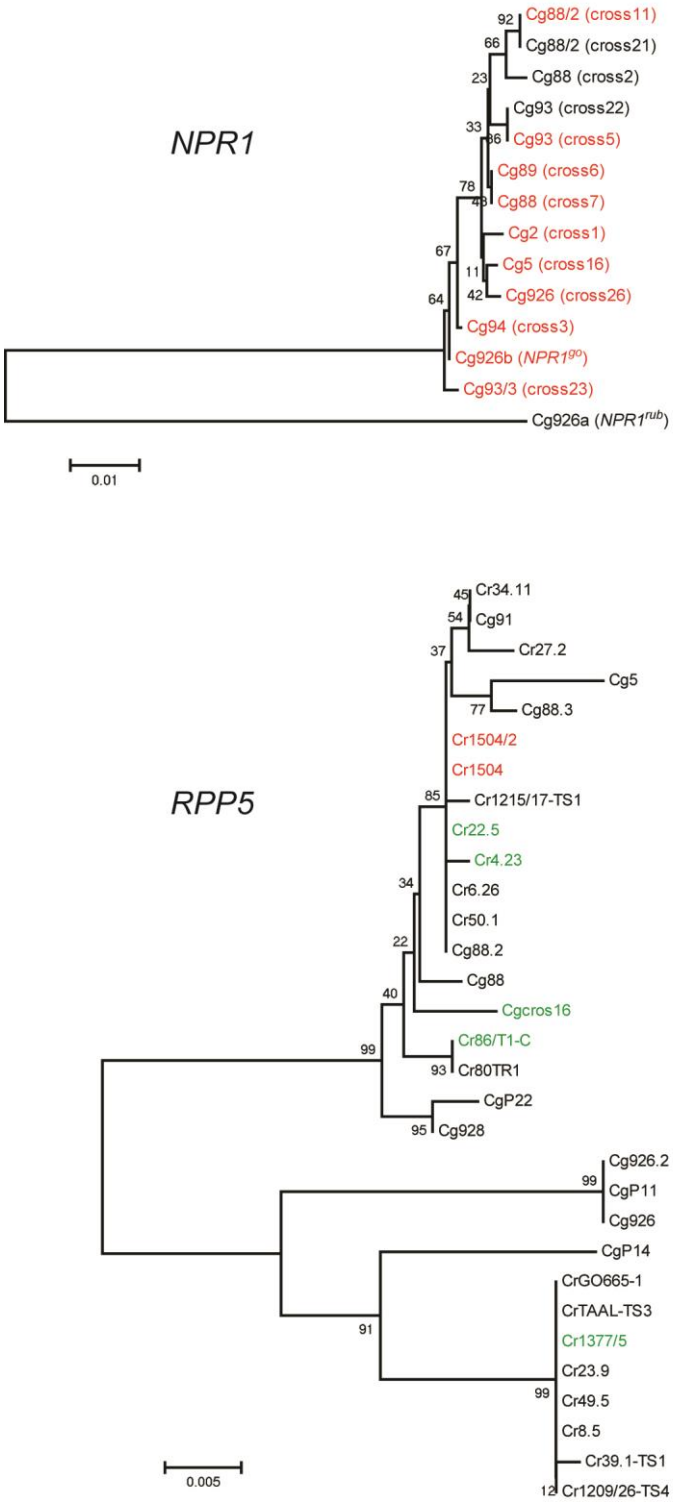


**Supplementary Figure 6: Extended *NPR1* and *RPP5* phylogenies.**

Phylogenetic trees for *NPR1* (top) and *RPP5* (bottom) including additional accessions used for crosses in Supplementary Figure 7. Incompatible haplotypes are indicated in red, compatible ones in blue and haplotypes not tested in grey. Analyses are based on resequencing of 700 bp (*NPR1*) and 800 bp fragments (*RPP5*). Numbers indicated bootstrap support from 1,000 runs. Red font indicates the alleles that have been tested in crossing experiments and shown to be incompatibles; green font

indicates alleles that have been tested in crossing experiments and shown to be compatible; and black font indicates the alleles that have not been tested.

**a**

| Cross number | *C. grandiflora* accession | *C. rubella* accession | F1 genotype* | % incompatible phenotype | *n* total | *n* strongly incompatible | *n* moderately incompatible |
|---|---|---|---|---|---|---|---|
| 1 | *Cg 2* | *Cr 1504/2* | *2gr;7gr* | 9.24 | 119 | 1 | 10 |
| 5 | *Cg 93* | *Cr 1504/2* | *2gr;7gr* | 22.12 | 113 | 7 | 18 |
| 6 | *Cg 89* | *Cr 1504/2* | *2gr;7gr* | 32.32 | 99 | 9 | 23 |
| 7 | *Cg 88* | *Cr 1504/2* | *2gr;7gr* | 10.26 | 117 | 0 | 12 |
| 11 | *Cg 88/2* | *Cr 1504/2* | *2gr;7gr* | 20.00 | 95 | 0 | 19 |
| 16 | *Cg 5* | *Cr 1504* | *2gr;7rr* | 8.30 | 253 | 0 | 21 |
| 23 | *Cg 93/2* | *Cr 1504* | *2gr;7gr* | 12.35 | 251 | 14 | 17 |
| 26 | *Cg 926* | *Cr 1504* | *2gr;7gr* | 25.00 | 148 | 8 | 29 |
| 30 | *Cg 926/2* | *Cr 1504* | *2gr;7gr* | 18.60 | 129 | 4 | 20 |
| 2 | *Cg 88* | *Cr 4.23* | *2gr;7gr* | 0 | 110 | 0 | 0 |
| 9 | *Cg 88/3* | *Cr 4.23* | *2gr;7gr* | 20.25 | 79 | 8 | 8 |
| 4 | *Cg 926/3* | *Cr 86IT1-C* | *2rr;7rg* | 0 | 97 | 0 | 0 |
| 12 | *Cg 926/4* | *Cr 22.5* | *2rr;7rg* | 0 | 119 | 0 | 0 |
| 21 | *Cg 88/2* | *Cr 22.5* | *2gr;7gr* | 3.88 | 103 | 3 | 1 |
| 3 | *Cg 94* | *Cr 1GR1-TS1* | *2gr;7gg* | 22.03 | 177 | 20 | 19 |
| 20 | *Cg 83* | *Cr 1GR1-TS1* | *2gr;7gg* | 0 | 132 | 0 | 0 |
| 24 | *Cg 88* | *Cr 1GR1-TS1* | *2gr;7gg* | 0 | 129 | 0 | 0 |
| 8 | *Cg 89* | *Cr 1377/5* | *2gr;7gr* | 0 | 126 | 0 | 0 |
| 10 | *Cg 5* | *Cr 1377/5* | *2gr;7gr* | 17.75 | 169 | 14 | 16 |
| 13 | *Cg 2h* | *Cr 1377/5* | *2gr;7gr* | 0 | 129 | 0 | 0 |
| 25 | *Cg 94* | *Cr 1377/5* | *2gr;7gr* | 0 | 135 | 0 | 0 |
| 27 | *Cg 5/2* | *Cr 1377/5* | *2gr;7gr* | 0 | 138 | 0 | 0 |

* for QTL2, "r" denotes an *NPR1rub* allele, "g" denotes an *NPR1go* allele; for QTL7, "r" denotes the presence of *RPP5*, "g" denotes its absence

**b**

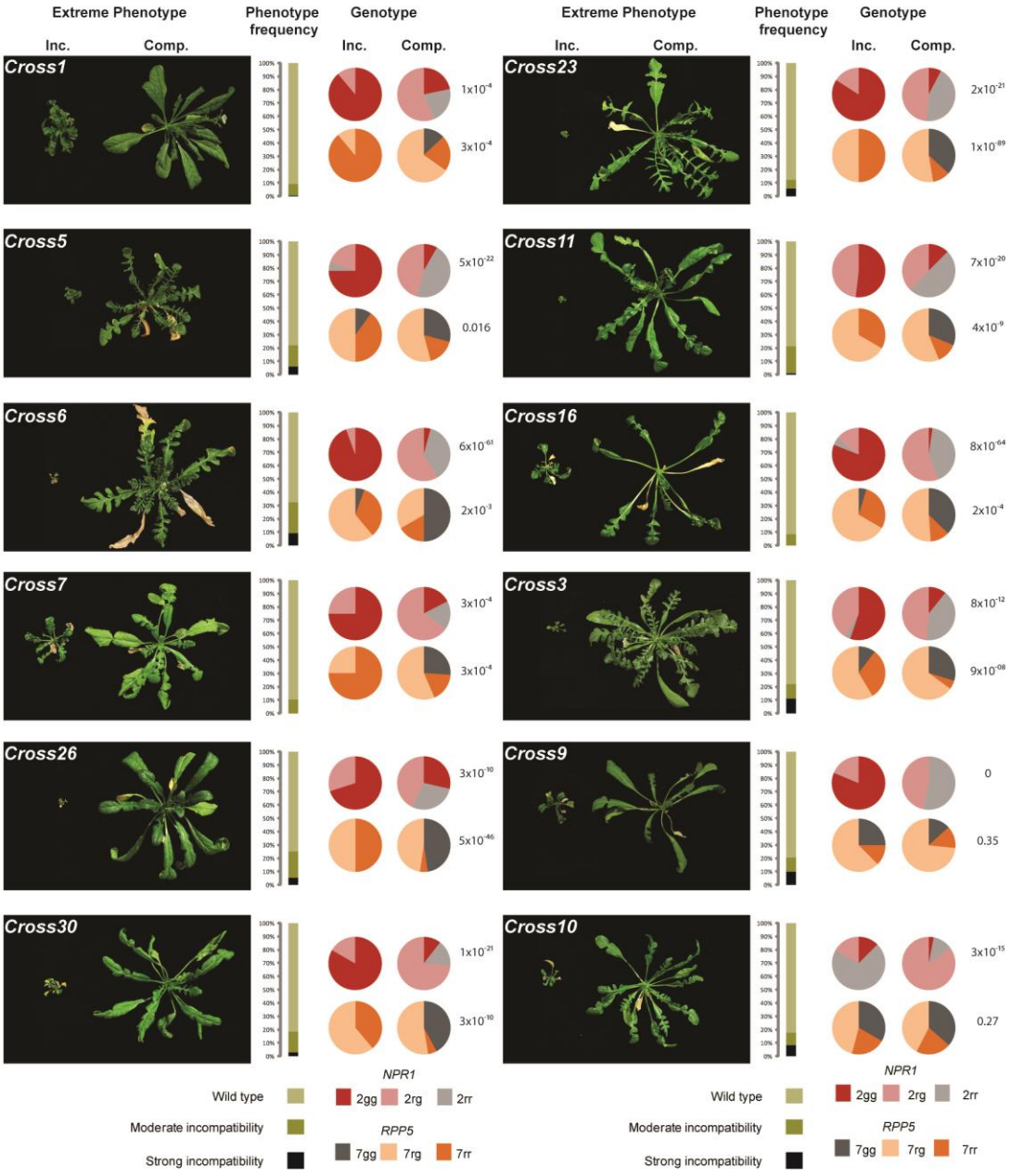

**Supplementary Figure 7: Incompatible phenotypes in additional *C. rubella* x *C. grandiflora* crosses.**

**a** Table of additional crosses performed and proportion of incompatible phenotypes in resulting F2 populations. Blue font indicates crosses in which no *RPP5* was segregating. Note that the absence of incompatible phenotypes in crosses 4 and 12 is not informative, as the *C. grandiflora* parental plants of these crosses did not pass on an $NPR1^{go}$ allele to the respective F1 plants. This is due to the *C. grandiflora* accession *Cg926* being heterozygous for $NPR1^{go}/NPR1^{rub}$ (see Fig. 3a).

**b** Phenotypes and genotypes of compatible and incompatible plants in F2 populations from crosses in (**a**). Numbers indicate the p-values determined by Chi-square test comparing genotype frequencies in the compatible and incompatible cohort. The sample size for the calculation of the phenotype frequency is indicated in figure 7a, n= 16 - 38 and n=8- 44 for the genotype frequency of the compatible and incompatible phenotypic classes respectively.

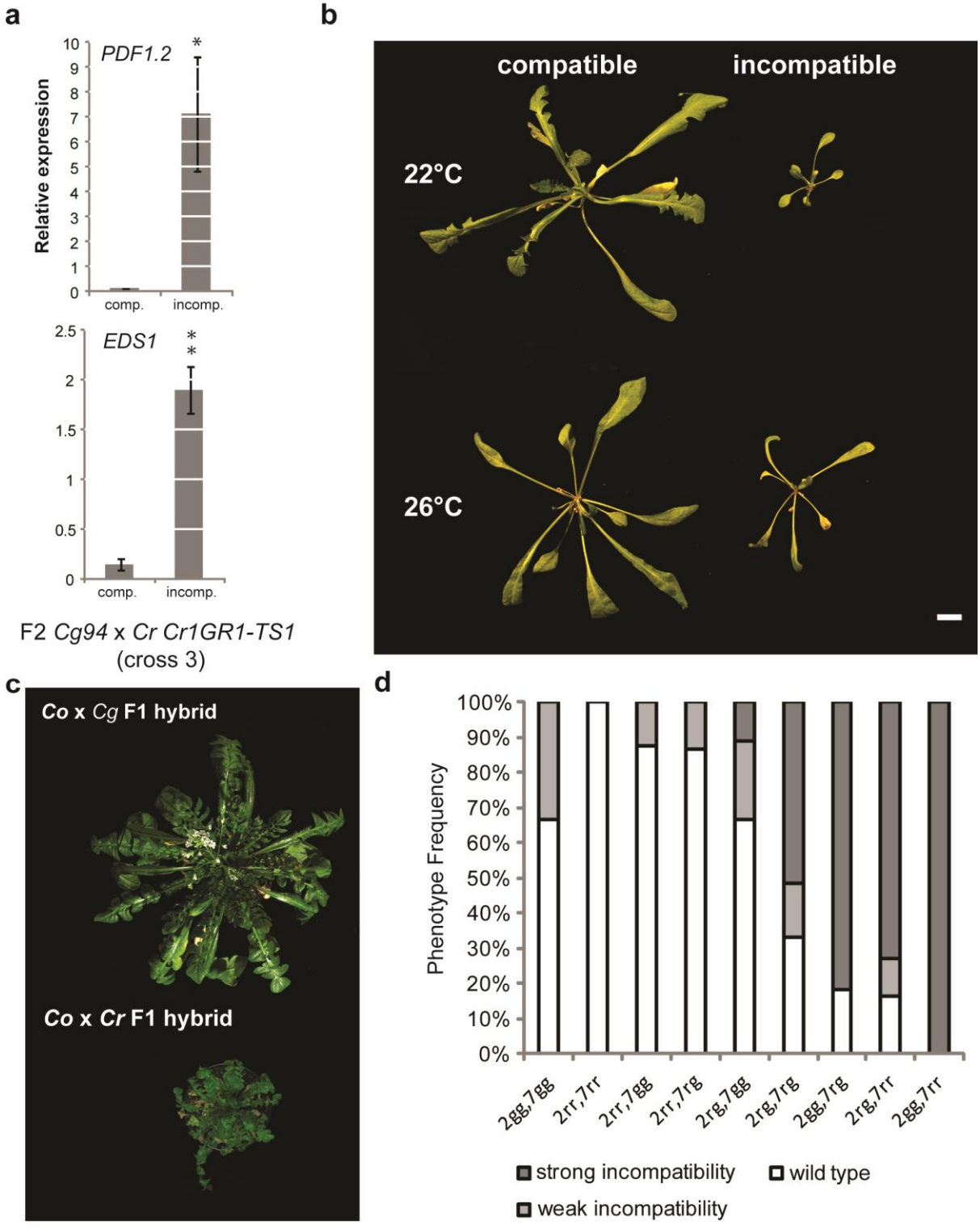


**Supplementary Figure 8: Characterization of an additional *NPR1*-linked, but *RPP5*-independent incompatibility between *C. grandiflora* and *C. rubella*, and of the incompatibility between *C. rubella* and *C. orientalis*.**

**a** Expression of the indicated immune-response markers determined by qRT-PCR normalized to *Capsella TUB6* in compatible and incompatible plants from cross 3 in Supplementary Figure 7. Mean

± s.e.m. of three biological replicates is shown. Asterisks indicate significant differences at * $p<0.05$ and ** $p<0.01$ based on a two tailed Student's t-test.

**b** Growth retardation in incompatible genotypes from cross 3 in Supplementary Figure 7 is alleviated by higher ambient temperatures.

**c** *C. orientalis Co1983* x *C. rubella Cr1504* (*Co* x *Cr*) F1 hybrids show an incompatible phenotype, whereas *C. orientalis Co1983* x *C. grandiflora Cg926* (*Co* x *Cg*) F1 hybrids do not.

**d** Phenotype distribution in different genotype classes of F2 plants from the *C. rubella 1504* x *C. orientalis* cross (n=144). For the *NPR1* genotype on chromosome 2, 'r' refers to the $NPR1^{rub}$ allele and 'g' refers to the $NPR1^{go}$ allele; for the *RPP5* genotype on chromosome 7, 'r' refers to the presence of *RPP5*, while 'g' refers to the deletion allele.

**a**

| Bin | Name | Elements | Odds ratio | P-value |
|---|---|---|---|---|
| 30.2.11 | signalling.receptor kinases.leucine rich repeat XI | 209 | 3.623193 | 0.0001604 |
| 29.4.1.57 | protein.postranslational modification.kinase.receptor like cytoplasmatic kinase VII | 318 | 2.6974307 | 0.0018602 |
| 29.4.1 | protein.postranslational modification.kinase | 326 | 2.62425436 | 0.0019645 |
| 20.1 | stress.biotic | 615 | 2.05602373 | 0.0038048 |
| 20 | stress | 1100 | 1.68163609 | 0.0154877 |
| 26.8 | misc.nitrilases, *nitrile lyases, berberine bridge enzymes, reticuline oxidases, troponine reductases | 102 | 3.69128104 | 0.0167027 |
| 29.4 | protein.postranslational modification | 1027 | 1.61747364 | 0.0488519 |

**b**

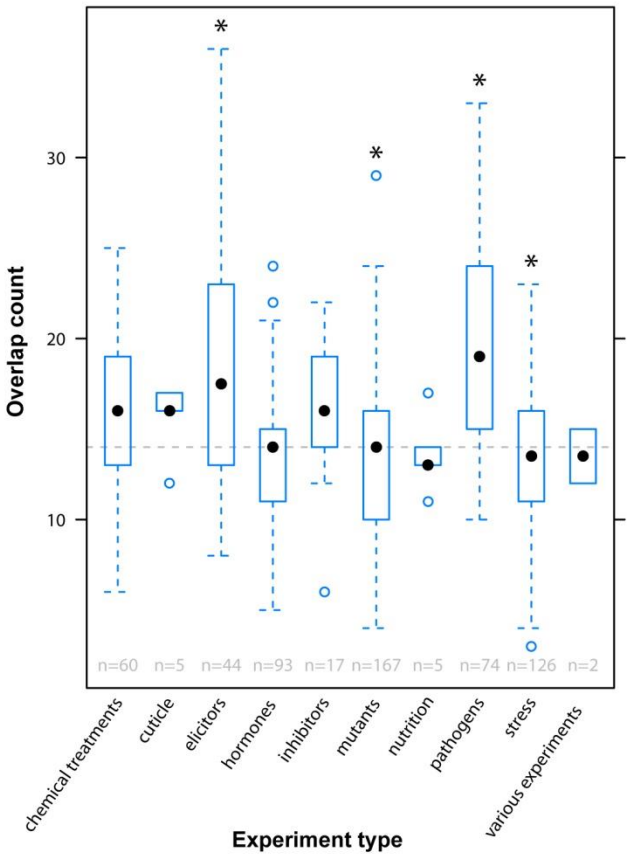


**c**

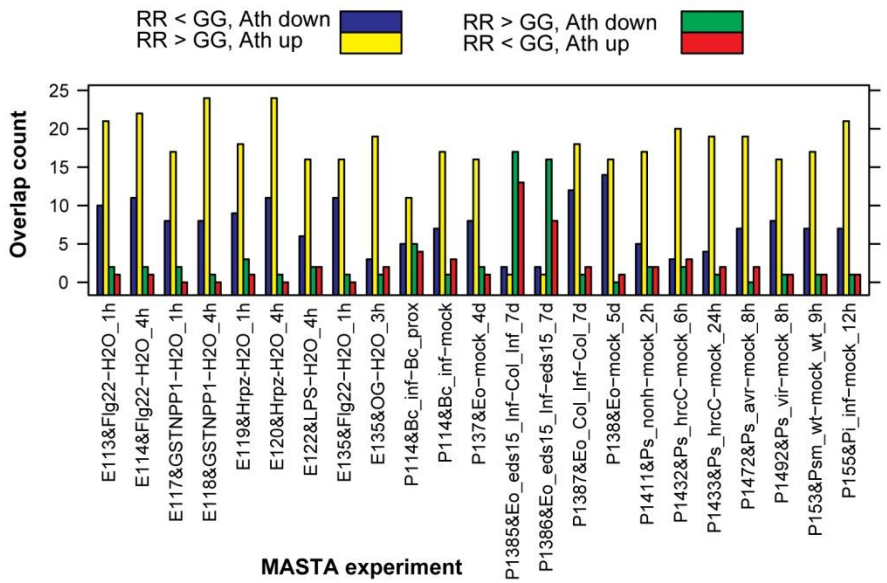

**Supplementary Figure 9: Transcriptome effects of different *NPR1* allele clades.**

**a** Table of overrepresented ($p<0.05$) MapMan categories amongst the 1000 genes with the lowest p-values when testing for association between gene expression and *NPR1* genotype. Categories were identified using a Fisher test. Bin and Name describe the categories, elements gives the number of genes of the category. P-values are BH corrected.

**b** Distributions of gene-overlap counts between the 1000 genes with the lowest p-values when testing for association between gene expression and *NPR1* genotype and *Arabiodpsis thaliana* microarray experiments grouped according to experiment type (n= 2-167). Overlaps were determined using MASTA; experiment type is based on MASTA classification. Asterisks mark significant difference from overlap counts with all experiments at $p<0.05$ based on Wilcoxon rank-sum test. n indicate the number of experiments per category. Pathogen experiments were the most strongly significant ones ($p<1e-11$) Dashed grey line represents median overlap for all experiments.

**Supplementary Table 1: Summary results of the QTL mapping for stunted growth in the *Cg926* x *Cr1504* RILs.**

| QTL | location in cM (closest marker) | LOD | 2LOD Confidece interval in cM (surronding markers) | Additive effect | Phenotypic variance explained (%) |
|---|---|---|---|---|---|
| QTL2 | 0 | 20.522 | 0-5 (cap5-1g63) | -0.36 | 41.261 |
| QTL7 | 35 | 11.694 | 30-45 (g06-g08) | 0.26 | 15.462 |

The additive effect was calculated as half of the difference of the phenotypic averages between Cr and Cg homozygote genotypes derived from the coding scheme +1 for Cr and -1 for Cg.

**Supplementary Table 2: Genotype of the near-isogenic line**

| Scaffold | Position (nt) | Marker (see ref. 1) | Genotype of NIL SAS437 (a: homozygous *C. grandiflora*; b: homozygous *C. rubella*; h: heterozygous) |
|---|---|---|---|
| 1 | 2299856 | A05 | b |
| 1 | 3114855 | A07 | b |
| 1 | 4555967 | A08 | b |
| 1 | 6168749 | A10 | b |
| 1 | 8858360 | A12 | h |
| 1 | 9766939 | 3G33 | b |
| 1 | 19167208 | A16 | b |
| | | | |
| 2 | 363608 | CAP5 | h |
| 2 | 403722 | B01 | h |
| 2 | 763403 | 1G63 | b |
| 2 | 955458 | B02 | b |
| 2 | 1587177 | 1G61 | b |
| 2 | 7388511 | B04 | b |
| 2 | 7816098 | B06 | b |
| 2 | 9064596 | B07 | b |
| 2 | 9604872 | B08 | b |
| 2 | 12200809 | B11 | b |
| 2 | 13270845 | B10 | b |
| | | | |
| 3 | 381439 | 3G02 | b |
| 3 | 6151596 | 3G17 | b |
| 3 | 7559574 | C004 | b |
| 3 | 13241733 | C06 | b |
| 3 | 13513239 | C10 | b |
| | | | |
| 4 | 1741932 | D03 | b |
| 4 | 7004190 | D04 | b |
| 4 | 7284563 | D05 | h |
| 4 | 8632170 | 2G32 | b |

| | | | |
|---|---|---|---|
| 4 | 13451362 | D08 | b |
| | | | |
| 5 | 34889 | C07 | h |
| 5 | 1824372 | E02 | h |
| 5 | 5274426 | E05 | h |
| 5 | 7709629 | E04 | h |
| 5 | 9974165 | E08 | h |
| 5 | 13584056 | CAP175 | b |
| | | | |
| 6 | 5967395 | F03 | h |
| 6 | 9368196 | F6 | a |
| 6 | 15009532 | 4G05 | b |
| 6 | 16513470 | F12 | b |
| 6 | 16525594 | F11 | b |
| | | | |
| 7 | 2298776 | G02 | b |
| 7 | 4512247 | G03 | h |
| 7 | 9972054 | 4G15 | h |
| 7 | 9569806 | G07 | h |
| 7 | 10149356 | G08 | h |
| 7 | 15915126 | G12 | b |
| 7 | 16968217 | G11 | h |
| | | | |
| 8 | 1078892 | H03 | b |
| 8 | 2623520 | H04 | b |
| 8 | 11130390 | H10 | b |
| 8 | 13265528 | H11 | b |

**Supplementary Table 3 : List of annotated genes in the mapping intervals.**

| QTL | Scaffold | Start | Stop | ID | *A. thaliana* homologues | Functional annotation |
|---|---|---|---|---|---|---|
| QTL2 | scaffold_2 | 202551 | 204786 | Carubv10021457m | AT1G64300.1 | Protein kinase family protein |
| | scaffold_2 | 211957 | 213051 | Carubv10021816m | AT1G64295.1 | F-box associated ubiquitination effector family protein |
| | scaffold_2 | 215677 | 216762 | Carubv10021907m | AT1G64290.1 | F-box protein-related |
| | scaffold_2 | 217298 | 219989 | Carubv10020031m | AT1G64280.1_ NPR1 | regulatory protein (NPR1) |
| | scaffold_2 | 220545 | 222704 | Carubv10020278m | AT1G64260.1 | MuDR family transposase |
| | scaffold_2 | 223775 | 225895 | Carubv10021357m | AT1G64260.1 | MuDR family transposase |
| | scaffold_2 | 227573 | 229999 | Carubv10021783m | AT1G64260.1 | MuDR family transposase |
| | scaffold_2 | 230895 | 233624 | Carubv10020053m | AT1G64255.1 | MuDR family transposase |
| | scaffold_2 | 234743 | 235063 | Carubv10021722m | AT1G64235.1 | Bifunctional inhibitor/lipid-transfer protein/seed storage 2S albumin superfamily protein |
| | scaffold_2 | 235451 | 237355 | Carubv10020996m | AT1G64230.1_UBC28 | ubiquitin-conjugating enzyme 28 |
| | scaffold_2 | 237595 | 238024 | Carubv10021245m | AT1G64220.1_TOM7-2 | translocase of outer membrane 7 kDa subunit 2 |
| | scaffold_2 | 238102 | 240015 | Carubv10021395m | AT1G64210.1 | Leucine-rich repeat protein kinase family protein |
| | scaffold_2 | 241053 | 242892 | Carubv10020883m | AT1G64200.1_VHA-E3 | vacuolar H+-ATPase subunit E isoform 3 |
| QTL7 | scaffold_7 | 9253104 | 9254894 | Carubv10005176m | AT4G08691.1 | |
| | scaffold_7 | 9254981 | 9258150 | Carubv10005361m | AT4G17050.1_ UGLYAH | ureidoglycine aminohydrolase |
| | scaffold_7 | 9257045 | 9262244 | Carubv10005166m | AT4G17040.1_CLPR4 | CLP protease R subunit 4 |
| | scaffold_7 | 9264180 | 9265793 | Carubv10005585m | AT4G17030.1_AT-EXPR | expansin-like B1 |
| | scaffold_7 | 9266354 | 9269322 | Carubv10006310m | AT4G17020.3 | transcription factor-related |
| | scaffold_7 | 9268573 | 9271765 | Carubv10005920m | AT4G17010.1 | |
| | scaffold_7 | 9272660 | 9275533 | Carubv10006518m | AT4G17000.1 | |
| | scaffold_7 | 9277237 | 9277809 | Carubv10006767m | AT4G16980.1 | arabinogalactan-protein family |
| | scaffold_7 | 9279776 | 9284122 | Carubv10004105m | AT4G16970.1 | Protein kinase superfamily protein |
| | scaffold_7 | 9291754 | 9296295 | Carubv10004008m | AT4G16890.1_BAL,SNC1 AT4G16950.1_RPP5 | disease resistance protein (TIR-NBS-LRR class), putative |
| | scaffold_7 | 9297395 | 9299037 | Carubv10005274m | AT4G16850.1 | |

| | | | | | |
|---|---|---|---|---|---|
| scaffold_7 | 9299185 | 9303240 | Carubv10004893m | AT4G16845.1_VRN2 | VEFS-Box of polycomb protein |
| scaffold_7 | 9303846 | 9304112 | Carubv10007592m | AT4G16840.1 | |
| scaffold_7 | 9304231 | 9306290 | Carubv10006791m | AT4G16835.1 | Tetratricopeptide repeat (TPR)-like superfamily protein |
| scaffold_7 | 9306420 | 9308554 | Carubv10005134m | AT4G16830.1 | Hyaluronan / mRNA binding family |
| scaffold_7 | 9309482 | 9311038 | Carubv10007507m | AT4G16820.1_PLA-Ibeta2 | alpha/beta-Hydrolases superfamily protein |
| scaffold_7 | 9316581 | 9318771 | Carubv10006259m | AT4G16810.1 | VEFS-Box of polycomb protein |
| scaffold_7 | 9321931 | 9324324 | Carubv10007038m | AT4G16810.1 | VEFS-Box of polycomb protein |
| scaffold_7 | 9325020 | 9327589 | Carubv10004885m | AT4G16807.1 | |
| scaffold_7 | 9328471 | 9329520 | Carubv10007120m | AT4G16800.1 | ATP-dependent caseinolytic (Clp) protease/crotonase family protein |
| scaffold_7 | 9332345 | 9334066 | Carubv10004732m | AT4G16790.1 | hydroxyproline-rich glycoprotein family protein |
| scaffold_7 | 9335010 | 9336719 | Carubv10005275m | AT4G16780.1_ATHB-2 | homeobox protein 2 |
| scaffold_7 | 9345932 | 9348909 | Carubv10005289m | AT4G16770.1 | 2-oxoglutarate (2OG) and Fe(II)-dependent oxygenase superfamily protein |
| scaffold_7 | 9349617 | 9353002 | Carubv10007744m | AT4G16770.1 | 2-oxoglutarate (2OG) and Fe(II)-dependent oxygenase superfamily protein |
| scaffold_7 | 9353682 | 9356075 | Carubv10006983m | AT4G16765.1 | 2-oxoglutarate (2OG) and Fe(II)-dependent oxygenase superfamily protein |
| scaffold_7 | 9357182 | 9361483 | Carubv10004312m | AT4G16760.1_ACX1,ATACX1 | acyl-CoA oxidase 1 |
| scaffold_7 | 9364548 | 9365366 | Carubv10005867m | AT4G16750.1 | Integrase-type DNA-binding superfamily protein |
| scaffold_7 | 9374054 | 9375936 | Carubv10007826m | AT4G16745.1 | Exostosin family protein |

**Supplementary Table 4**: **Geographic origin of the additional *C. grandiflora* populations collected during this study.**

| ***C. grandiflora* population** | **City, country** | **Latitude/Longitude** |
|---|---|---|
| *P19* | Kastanonas, Greece | 39,84N/20.95E |
| *Cg 926/2* | Votonosi, Greece | 39.76N/21.11E |
| *P18* | Vovusa, Greece | 39.91N/21.05E |
| *P11* | Metsovo, Greece | 39,77N/21,18E |
| *P14* | Metsovo, Greece | 39.76N/21.18E |
| *P22* | Konitsa, Greece | 40.05N/28.89E |

**Supplementary Table 5: List of the primers used in the study**

| Name | Usage | Position; Polymorphism *Cr/Cg* | Sequence (5'-3') |
|---|---|---|---|
| oAS1036 | Cloning of NPR1 ORFs | n.a. | TTAATTAA ATGGACACCAATCTTGATGGATTCGC |
| oAS1037 | Cloning of NPR1 ORFs | n.a. | TTAATTAATCACCGACGCCGATTAGAGAGTT T |
| oAS1137 | Cloning of the 173tsRPP5 | n.a. | CTCCTCTTAATTAAGTGATTTTTCTCTACAAG CGAATCTAGAGAGGATATTCGAGAAGTATTG ACCGATA |
| oAS1138 | Cloning of the 173tsRPP5 | n.a. | CTCCTCTTAATTAATTGAGACTTCCAAGTCGC AGAGTTCC |
| oAS1129 | Genotyping of NPR1 | n.a. | TTGATGCTCTTCTAGGATTTTGAAAGGTGCTA |
| oAS1130 | Genotyping of NPR1 | n.a. | GACTCGGATGATATCACGCTAGTCAATTTGC |
| oAS873 | Genotyping CrRPP5 | n.a. | CAAACCATAATAGTAAGATGCTTCAGTTACC AG |
| oAS1123 | Genotyping CrRPP5 | n.a. | TCGAATACCTCGATCTCAGTGGTT |
| oAS839 | genotyping CgRPP5 | n.a. | GCTGTTGATGCTTAAGGAGGTTCCC |
| oAS1133 | genotyping CgRPP5 | n.a. | GTTAATGATGGGAAGAACACCTTTTAC |
| oAS1276 | genotyping CgRPP5 | n.a. | ATGAAAATCTCCACTCAAGTAGTGTCCACAC |
| oAS1072 | qPCR *CaNPR1* | n.a. | CACCGAGTCCTCTATCGTTTATC |
| oAS1073 | qPCR *CaNPR1* | n.a. | GTCAGCGAGAACGAGCTTAG |
| oAS1084 | qPCR *caTUB6* | n.a. | GCTCCTTCAGTGTAGTGCCC |
| oAS1085 | qPCR *caTUB6* | n.a. | CAGAACTGGCCCTTATGGTC |
| oAS1068 | qPCR *CaRPP5* | n.a. | GACGATGAGATTAAAATGACTTCTGCCA |
| oAS1069 | qPCR *CaRPP5* | n.a. | AGCGCCTTGAGAAGATGACTAAGGAA |
| oAS1145 | qPCR *Carubv10025432m* | n.a. | GTAACCTGTACCAATTTGTACCCATC |
| oAS1146 | qPCR *Carubv10025432m* | n.a. | TGTAGAGATGCCATCCTGGCG |
| oAS1074 | qPCR *CaPR1* | n.a. | TTGCAACTGATGATGGTTCC |
| oAS1075 | qPCR *CaPR1* | n.a. | TAGTGGCGACTTGTCTGGTG |
| oAS1111 | qPCR *CaEDS5* | n.a. | TCTTTATTGGTTTGGTTTGTGG |
| oAS1112 | qPCR *CaEDS5* | n.a. | CAGTAACAGCCCAAGGTCC |
| oAS1113 | qPCR *CaEDS1* | n.a. | TCGGAAGGAGAAATACACGG |
| oAS1114 | qPCR *CaEDS1* | n.a. | GCTCTTACCGGAATCAATGG |
| oAS1078 | qPCR *CaPDF1.2* | n.a. | TTATGCGAGAGGTCAAGTGG |
| oAS1079 | qPCR *CaPDF1.2* | n.a. | GATCCATGTCGTGCTCCTTC |
| oAS1107 | qPCR *PR2* | n.a. | TCTCAGACACCCCGATCTTC |
| oAS1108 | qPCR *PR2* | n.a. | CCACATGTATAACTCGGGCC |
| oAS1109 | qPCR *CaPAD4* | n.a. | AAGAAAGGCAGCACATAGATCC |
| oAS1110 | qPCR *CaPAD4* | n.a. | ACAAAGCTCGCGAAGAGAAG |
| oAS1080 | qPCR *CaORA59* | n.a. | ACCGCCCTAGAGGAAAGAAG |
| oAS1081 | qPCR *CaORA59* | n.a. | TCACTTTCTTGCGTCGTGAC |
| oAS928 | HiB1 CAPS markers using *HindII* | scaffold_2:75028; C/T | GGTTCGTCGGCGCACACATTGAG |
| oAS929 | HiB1 CAPS markers using *HindII* | | CTCACTTCTCAATCTCTCTCGGTAATG |

| | | | |
|---|---|---|---|
| oAS926 | HiB2 dCAPS markers using *ClaI* | scaffold_2:129775; C/T | TCGAACGGCAATCTTCAAGTTCATCGA |
| oAS927 | HiB2 dCAPS markers using *ClaI* | | CTATTCTCGACGACGAGCTTCTAAG |
| oAS1001 | HiB3 CAPS markers using *NlaIII* | scaffold_2:203131 ; A/G | AGTCAGAAGCAGGACCAGAGAGTTGTC |
| oAS1002 | HiB3 CAPS markers using *NlaIII* | | CACACCTGATCCTATAATCTGGTATGCAC |
| oAS1039 | HiB4 CAPS markers using *DdeI* | scaffold_2:241249 ; G/A | AACCAGATCCACCAGATGGTCTGCT |
| oAS1040 | HiB4 CAPS markers using *DdeI* | | AAGATCAAGATCAAGAGAGAGAGAAGAATT |
| oAS991 | HiB5 CAPS markers using *ApoI* | scaffold_2:249356 ; C/T | CGGTTCAGTACTTTAAGAAGTTCGGTT |
| oAS992 | HiB5 CAPS markers using *ApoI* | | GTTCTGGAATTTCCCAATTGCTCTG |
| oAS917 | HiB6 CAPS markers using *AluI* | scaffold_2:252505 ; G/C | TAGTGACATTGACATAGAAGAGTGATGGG |
| oAS918 | HiB6 CAPS markers using *AluI* | | GTGTGACTCTAGCATAAGGTATTGTAAGCTC |
| oAS916 | HiB7 dCAPS markers using *DdeI* | scaffold_2:303580 ; G/A | ACAAGTGGGCAGACAAGCCACTCA |
| oAS910 | HiB7 dCAPS markers using *DdeI* | | CTTACCGTATCATTTTCAAGAACATGACAGA |
| CAP5_F | HiB8 dCAPS markers using *PstI* | scaffold_2:363608 ; G/T | TCACCTCTTTGGTCACACTGCA |
| CAP5_R | HiB8 dCAPS markers using *PstI* | | TGGATTGCGTGATTTTGTT |
| oAS797 | HiG1 CAPS markers using *TaqI* | scaffold_7:8868399 ; G/A | CTCAATGGTGCAGTTACATCAAACTCTC |
| oAS798 | HiG1 CAPS markers using *TaqI* | | AATGTGGTGCATTTAGGCAACAGC |
| oAS808 | HiG2 dCAPS markers using *DdeI* | scaffold_7:9135785 ; A/G | ACAAGAATGGGGACAATGGATAACC |
| oAS809 | HiG2 dCAPS markers using *DdeI* | | GAATCGTGATATCGTATCTCTCATTTG |
| oAS810 | HiG3 dCAPS markers using *XcmI* | scaffold_7:9106757 ; A/G | AGCTGGAGAACAGTTCTGTGTCACT |
| oAS811 | HiG3 dCAPS markers using *XcmI* | | TTTTTGGAATTGCATCCATGGAAGTAT |
| oAS1249 | HiG4 Indel markers | scaffold_7.9253895; GAAAGGGAGTTAGGAG/TAAGCTAAACTCCAGGGTTCGANNNNNNNNNNTGTTTTACTTGGGTGCAGTTGG | AAGCTAAACTCCAGGGTTCGA |
| oAS1250 | HiG4 Indel markers | | TGTTTTACTTGGGTGCAGTTGG |
| oAS806 | HiG5 CAPS markers using *XmnI* | scaffold_7:9374725 ; A/C | CGTTGCAGAGAGCTTTAATAGAATTTC |
| oAS807 | HiG5 CAPS markers using *XmnI* | | GTCGCTTGCCACGATTGGGTAATA |
| G07_F | HiG6 CAPS markers using *HinfI* | scaffold_7:9569807 ; C/T | AAGGATGCTGTCAGCTGCCTTCTTG |
| G07_R | HiG6 CAPS markers using *HinfI* | | TGGATACAGGTGGCCTATGGTGTC |

n.a. not applicable

## Supplementary Discussion

### Genetic incompatibilities in the genus *Capsella*.

The genetic incompatibility in the *Cr1504* x *Cg926* RIL population suggested that the presence within the same cells of RPP5 and NPR1$^{go}$ induces an autoimmune response. If true, any crosses combining a functional RPP5 protein with NPR1$^{go}$ should recreate the stunted growth phenotype. We tested this hypothesis by performing random crosses between seven *C. rubella* and nine *C. grandiflora* accessions (Supplementary Fig. 7). A phenotype similar to the *Cr1504* x *Cg926* incompatible hybrids was segregating in 13 of the resulting $F_2$ populations.

The *RPP5* alleles from three of the *C. rubella* accessions used for the crosses (*Cr4.23*, *Cr86IT1-C* and *Cr1377/5*) belong to different haplotype groups than *Cr1504RPP5* (Supplementary Fig. 5b), while no *RPP5* could be detected in a fourth *C. rubella* accession (*Cr 1GR1-TS1*). Among the *C. grandiflora* x *C. rubella* $F_2$ progenies descending from these *C. rubella* accessions, we did not observe any correlation between the *RPP5* genotype (as determined by a tightly linked molecular marker HiG2 to be able to assess the genotype at the *RPP5* locus also in progeny of *Cr 1GR1-TS1*) and the stunted growth. Similarly, no correlation was observed in the $F_2$ population descending from *Cr22.5* in cross 21, whose *RPP5* allele belongs to the same haplotype group as *Cr1504RPP5*. We note that the absence of incompatible phenotypes in cross 12, also involving *Cr22.5*, and in cross 4 is not informative, as the *C. grandiflora* parental plants of these crosses did not pass on an *NPR1$^{go}$* allele to the respective F1 plants. This is due to the *C. grandiflora* accession *Cg926* being heterozygous for *NPR1$^{go}$/NPR1$^{rub}$* (see also Fig. 3a). In fact, a robust correlation between incompatible phenotype and *RPP5* genotype was only seen in $F_2$s descending from crosses between *Cr1504* and diverse *C. grandiflora* individuals. These results indicate that only a specific *RPP5* haplotype is incompatible with the *NPR1$^{go}$* alleles. It is therefore likely that after the divergence of *C. rubella* from *C. grandiflora*, a novel mutation in *Cr1504RPP5* has rendered it incompatible with *NPR1$^{go}$*. This hypothesis is supported by the observation that no correlation between stunted growth phenotypes and *RPP5/NPR1* genotypes was observed within natural *C. grandiflora* populations.

In addition, modifier alleles of the *NPR1/RPP5* incompatibility appear to be segregating in *C. grandiflora*. This is based on the observation that the strength and frequency of the stunted growth varies between the different $F_2$s descending from *Cr1504*. For example, although the same *NPR1$^{go}$* and *RPP5* haplotype are segregating in the crosses 6 and 7, only 10 % of the

$F_2$s show an incompatible phenotype in cross 7 versus 30% in cross 6 (Supplementary Fig. 6A,S7), and the phenotypic severity is reduced in the cross 7 relative to the cross 6 $F_2$ progenies (Supplementary Fig. 7B). Since *Cr1504* is highly inbred, this indicates that modifiers affecting the penetrance and expressivity of the genetic incompatibility are segregating within *C. grandiflora*.

Importantly, we observed that $NPR1^{go}$ haplotypes are also associated with genetic incompatibilities that do not involve *RPP5* (Supplementary Fig. 7; crosses 3 and 9). In the progeny of cross 9, all plants homozygous for the $NPR1^{go}$ allele showed the incompatible phenotype, while none of the plants homozygous for $NPR1^{rub}$ did so, yet there was no difference in the *RPP5* genotype frequency between plants with incompatible and compatible phenotypes. Similarly, in the $F_2$ of cross 3, in which no *RPP5* presence could be detected, all but one of the 39 incompatible hybrids had at least one copy of the $NPR1^{go}$ allele, and $NPR1^{go}$ homozygotes were underrepresented amongst compatible plants. Individual $NPR1^{rub}$ homozygotes amongst the incompatible plants were also observed in two of the crosses involving *Cr1504*, which is likely due to mis-scoring of the phenotype or to unrelated deleterious mutations from the *C. grandiflora* parent that became homozygous in the $F_2$. Given also the molecular evidence for a constitutive auto-immune response in the incompatible plants in the $F_2$ from cross 3 (Supplementary Fig. 8a,b), we consider it highly likely that this incompatibility is also caused by the $NPR1^{go}$ allele. In the $F_2$ of cross 10, the stunted growth phenotype co-segregated with the $NPR1^{rub}$ allele, but not with the *RPP5* genotype (Supplementary Fig. 7). While suggestive of an involvement of $NPR1^{rub}$ in the incompatibility, several incompatible plants were homozygous for $NPR1^{go}$, and further experiments will be needed to test a causal role for $NPR1^{rub}$. In any case, these results indicate that alleles at additional loci are incompatible with $NPR1^{go}$ and possibly $NPR1^{rub}$; these alleles are likely to segregate in *C. grandiflora*, as the incompatibilities were only observed in some, but not all crosses involving a given *C. rubella* accession (compare for example crosses 3, 20 and 24). Together, these results support the notion that the two *NPR1* haplotype groups with their strong sequence divergence resulting from long-term balancing selection facilitate the establishment of genetic incompatibilities by mutations to interacting loci. If any such strongly divergent haplotypes were sorted into derived populations in a mutually exclusive manner, for example following genetic bottlenecks such as during independent transitions to selfing from an ancestral outbreeding species, the first step to the formation of a gene-flow barrier would already have been achieved, and only one further

mutation to an interacting locus in one of the derived populations would be required for the establishment of a BDMI.

**Supplementary Reference**

1. Sicard, A. *et al.* Genetics, evolution, and adaptive significance of the selfing syndrome in the genus Capsella. *Plant Cell* **23**, 3156-3171 (2011).